Observation of a Bi-Domain State and Nucleation Free Switching in Mesoscopic Ring Magnets

J. Rothman,[1] M. Kläui,[1] L. Lopez-Diaz,[1] C. A. F. Vaz,[1] A. Bleloch,[1] J. A. C. Bland,[1] Z. Cui,[2] and R. Speaks[3]

[1]*Cavendish Laboratory, University of Cambridge, Madingley Road, Cambridge CB3 0HE, United Kingdom*

[2]*Rutherford Appleton Laboratory, Chilton, Didcot OX11 0QX, United Kingdom*

[3]*Department of Material Science and Metallurgy, University of Cambridge, New Museums Site, Pembroke Street, Cambridge CB2 3QZ, United Kingdom*

(Received 3 August 2000)

We present the results of a study of the magnetic properties of an array of 34-nm thick Co(100) epitaxial ring magnets, with inner and outer diameters of $d_{in} = 1.3$ μm and $d_{out} = 1.6$ μm, respectively. Magnetic measurements and micromagnetic simulations show that a two step switching process occurs at high fields, indicating the existence of two different stable states. In addition to the vortex state, which occurs at intermediate fields, we have identified a new bi-domain state, which we term the onion state, corresponding to opposite circulation of the magnetization in each half of the ring. The onion state is stable at remanence and undergoes a simple and well characterized nucleation free switching.

DOI: 10.1103/PhysRevLett.86.1098 PACS numbers: 75.60.Ej, 75.60.Ch, 75.70.Ak, 85.70.Kh

Understanding the magnetic properties of small magnetic elements is a major challenge in fundamental physics, involving both the static and the dynamic properties, as well as for technological applications, such as high density magnetic storage. The key issue is to control the magnetic switching precisely. To achieve this one needs first to have a well defined and reproducible remanent state, and second the switching process itself must be simple and reproducible. Different geometries have been studied for this purpose, going from simple circular disks [1,2] to more advanced needle shape elements [3]. In such topologically simply connected elements, the aim is to obtain a single-domain state and switching by coherent rotation [4]. However, because of the demagnetizing field induced by dipole interactions, the magnetization direction will always change close to the borders [1,5] to form edge domains. The magnetic configurations in these elements will therefore be defined by the shape of the edges and will be very sensitive to shape fluctuations and edge roughness. The edge inhomogeneity in the magnetization will dominate the magnetic properties, acting as nucleation sites for what is, in general, a complicated nucleation propagation switching process, where the magnetization passes through inhomogeneous intermediate states. The complex switching mechanism can lead to different remanent states depending upon the applied field history and hence influence the switching itself. One possible way to overcome these complications in circular elements is to use the vortex state in which the magnetic flux is closed in the element and where the edge roughness and edge domains play a minor role. The zero stray field in this state will also favor high density storage. However, the vortex is stable only in disks for diameters above 100 nm [2], depending on the thickness and the material, which limits the density achievable. Moreover the vortex formation is complex and hard to control [2,6]. The vortex state can be made more stable if the highly energetic vortex core is removed by using a ring element [7], which has also been proposed for use in magnetic random access memories [8]. In this Letter we present an experimental and computational study of an array of epitaxial fcc-Co(100) rings, having an outer diameter $d_{out} = 1.6$ μm, an inner diameter $d_{in} = 1.3$ μm, and a thickness of 34 nm. These mesoscopic rings were deliberately chosen to be narrow, i.e., having a small difference between the inner and outer diameters, since particularly simple magnetic states, in addition to the vortex state, are expected in this case.

The rings were obtained by depositing a trilayer Cu(100)/Co(100)/Cu(100) on a Si(100) wafer in a UHV molecular-beam-epitaxy system (base pressure 3×10^{-10} mbar). Before deposition, the Si was patterned into the desired shape. Rings were first patterned on a resist layer by electron beam lithography using a Leica EMBL-300 system at 50 keV. The resist was then used as a mask to etch the silicon with a reactive ion etching system from Oxford Plasma Technology, defining slightly undercut structures with a flat summit and rough surrounding trenches. The height of the structures was varied between 150 and 700 nm. The use of isotropic etching means that the elements obtained after etching are smaller than what was defined during lithography, as the structures are also etched from the side. Hence, this method opens the way to obtaining structures smaller than the resolution of the lithography, possibly below 10 nm. A key advantage of structures on prepatterned substrates is that, in contrast to conventional methods, no damage to the magnetic material is introduced by the patterning process. A fcc Cu layer was grown directly on the patterned Si after HF cleaning. To obtain a high quality Cu crystal, a 65-nm thick buffer layer was grown at ambient temperature [9]. The Cu ($t = 20$ Å) and Au ($t = 40$ Å) capping layers were also grown at ambient temperature. The last 20 Å of Au was grown under non-normal incidence, typically 45°, and rotation which gives a lateral protection from oxidation, in contrast with the case of etched or lift-off structures.

 0031-9007/01/86(6)/1098(4)$15.00

A top view of one of the studied rings before deposition is shown in Fig. 1(a). The image reveals that both a significant asymmetry and edge roughness exist, the latter due to the fast etching of the Si. A side view of a ring after deposition of the epitaxial layers, with a Co thickness of 34 nm is shown in Fig. 1(b). We note that the surface on the top of the ring is flat, which shows that the magnetic rings have a thin-film shape. A concern with these samples is the magnetic coupling between the desired magnetic structures on the summits and the magnetic material in the trenches. This coupling is mainly dipolar, resulting from the stray field at the edge of the trenches, but direct exchange coupling can also arise if the Co on the summits is physically connected to the Co in the trenches. The edge of the metallization in the trenches can be observed on the side of the structure [Fig. 1(b)], indicating that the Co on the summit is disconnected from the trenches. Combined scanning transmission electron microscopy (STEM) and electron energy loss spectroscopy (EELS) studies were performed to further investigate the growth and the geometrical definition of the structures. The STEM-EELS measurements were performed with a Vacuum Generators HB501-STEM on a 440 nm diameter and 170 nm high disk, initially milled into a 100 nm slice by focused ion beam milling. In Fig. 2 we show a STEM micrograph of the structure. The use of EELS permits a quantitative determination of the local stoichiometry, as indicated in the figure. The studies show that a special growth mode of the fcc-Cu(100) occurs on the Si(100) which helps to define the structures: the Si pillars are initially undercut and the Cu continues to grow overhanging in the same direction. When the Co is deposited, the edge profile changes slope, defining a trapezoid shaped cross section. The EELS measurements have proved quantitatively that no direct exchange between the Co on the summits and in the trenches exists.

Magnetic measurements on these prepatterned structures is a challenge as most of the sample is occupied by unwanted magnetic material in the trenches. Magneto-optical Kerr effect (MOKE) measurements can be used due to the difference in polarization of the light reflected from the trenches and the summits which originates from interference and roughness effects [10]. A maximum signal from the summits can be obtained by adjusting the analyzer to extinction for the signal from the trenches. To further enhance the magnetic signal from the summits, a light absorbing resist (Brewer Science PSK 2000) was spun on the sample to cover the trenches. The measurement with optimized signal from the array of rings is presented in Fig. 3(a). The open circles represent the magnetic signal from the rings, where the contribution from the trenches has been subtracted from the measured signal, shown by the crosses. Two transitions in high fields, labeled (1) and (2), are observed, with an average switching field of $\langle H_{C1}\rangle = 435$ Oe and $\langle H_{C2}\rangle = 946$ Oe. Hysteresis loops measured along and between the easy and the hard cubic magnetocrystalline anisotropy axes show no difference in the switching behavior. Minor loops starting from saturation in one direction were performed to investigate the nature of the two transitions and to estimate the irreversible susceptibility. The diamonds in Fig. 3(a) represent a minor loop where the maximum positive applied field was intermediate between the two transition fields. We note that the change of the magnetization is very small away from the transition and that the remanence is zero. The reverse transition occurs at an applied field corresponding precisely to $-H_{C2}$. This shows that the transition (1) is a switch from the first stable state into a second stable state. The second state has zero remanent magnetization, and subsequently switches back to the first state independently of the applied field direction. From this we conclude that this second state must correspond to the vortex state. Further, minor loops for smaller maximum positive applied field than that used in the minor loop in Fig. 3(a) show the same transitions. Therefore, all irreversible processes in the vicinity of H_{C1} correspond to direct transitions into the vortex state without stable intermediate states. The measured irreversible susceptibility is shown in Fig. 3(b) and is seen to be zero before the first transition. Hence, the first state

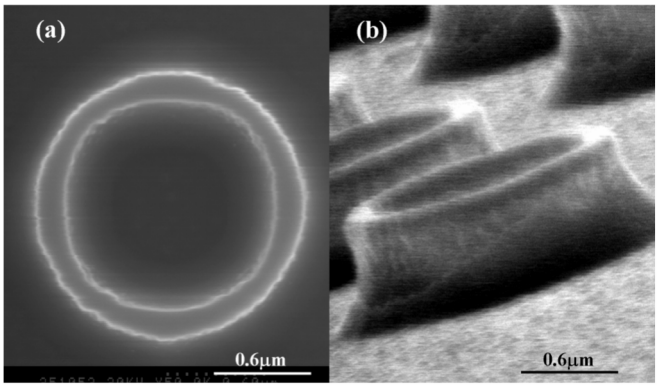

FIG. 1. SEM micrographs of rings (a) before and (b) after deposition. Because of fast etching of the Si, the ring possesses a significant edge roughness and asymmetry, which influences the magnetic properties of the ring (a). The flat surface on the top of the rings and the edge of the metallization on the side of the structures indicate that the rings are well defined (b).

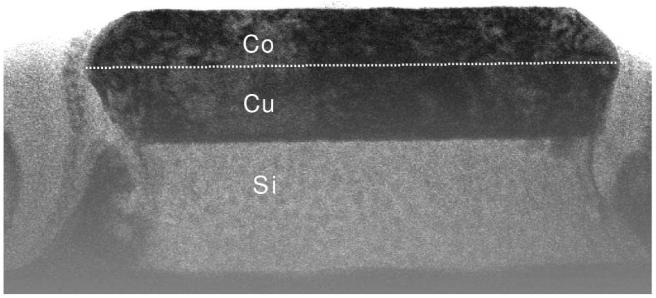

FIG. 2. Cross-sectional STEM micrograph after growth on a 440 nm diameter 170 nm high Si(100) pillar. The chemical identification was obtained using EELS. The light contrast material around the pillar was redeposited during the ion milling.

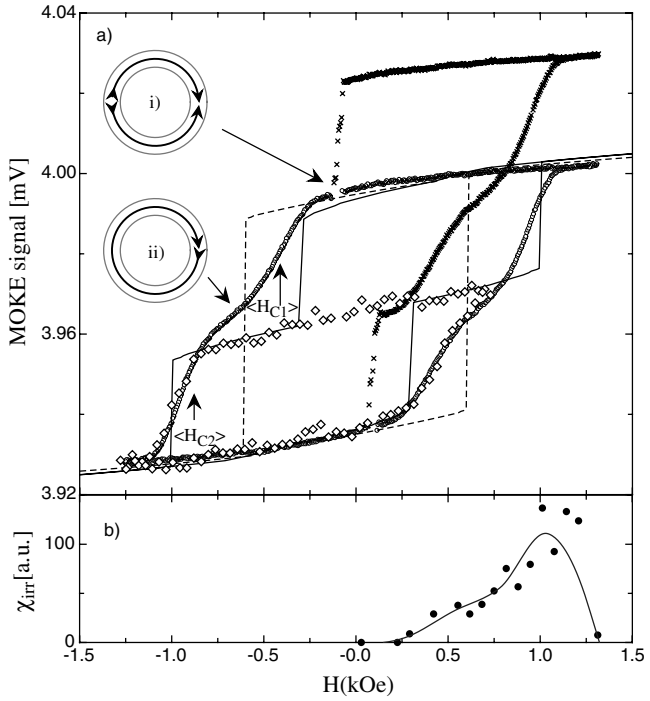

FIG. 3. (a) Hysteresis loops of $d_{\text{in}}/d_{\text{out}} = 1.3/1.6$ μm epitaxial ring magnets. The open circle curve is the corrected loop for the rings obtained from the measured MOKE data (crosses). The dashed and solid lines represent the simulations of a symmetric ring and an asymmetric ring, respectively. The cartoons are schematics of (i) the onion state and (ii) the vortex state, which occur as indicated by the arrows. The diamonds represent an asymmetric minor loop achieved from saturation in negative fields. (b) The measured irreversible susceptibility: for each minor loop obtained at a given maximum field H_{max}, the irreversible change in the magnetization ΔM_{irr} was determined. The quantity $d\Delta M_{\text{irr}}/dH_{\text{max}}$ provides an estimate of the irreversible susceptibility χ_{irr}. The continuous line is a guide to the eye.

is reached reversibly from saturation. This implies that as the field is decreased the flux must be closed on each half of the ring defining a state with two opposing head-to-head walls, as schematically represented in the figure. We will from now on refer to this state as the onion state, due to its resemblance to the cross section of an onion when it is cut from top to bottom. The two transitions indicated in Fig. 3(a) can therefore be described as (1) onion to vortex state and (2) vortex to the reverse onion state. We note that the distribution of switching fields is rather wide for the two transitions with a standard deviation of 170 Oe and 100 Oe, respectively. The origin of these distributions will be discussed later.

To gain further insight into the switching process we have performed micromagnetic simulations. Two different geometries were considered, one symmetric ring and one asymmetric ring, and were used to simulate the effects of shape fluctuations. Hysteresis loops were computed by solving the micromagnetic equilibrium equation for each applied field on a 2D square mesh, with a 5 nm cell size. A conjugate gradient solver was used for the energy minimization [7]. The intrinsic parameters used are the following: $M_S = 1.424 \times 10^6$ A/m, $A = 3.3 \times 10^{-11}$ J/m, and $K_1 = 6.5 \times 10^4$ J/m^3.

The hysteresis curves obtained from the simulations are compared to the experimental results in Fig. 3. For the symmetric ring we observe only one transition: the ring switches directly from one onion to the reverse onion state without going into the vortex state. The switching mechanism in this case is surprisingly simple and close to coherent rotation. The two walls start to move simultaneously in the same rotational direction so that they chase each other around the perimeter of the ring. The onion state is completely switched when the walls have reached the opposite side. However, if any asymmetries are present in the ring, as in our experiments, the simulations show that the walls will not start to move simultaneously. One wall will be more strongly pinned than the other, and a transition into a vortex state will take place when the other wall has depinned and moved to the pinned wall, which results in the annihilation of both walls. This is illustrated in Fig. 3, where two transitions are observed for the asymmetric ring. Figure 4 shows snapshots of the first transition in Fig. 3. The simulated switching field for the onion to vortex transition, $H_{C1} = 350$ Oe, falls well within the distribution of the experimental values. We note that the walls in the onion state are head-to-head vortex walls as shown in Fig. 4(a). For narrower or thinner rings the walls will be transverse walls just as occurs in thin magnetic strips [11]. It is expected that the precise nature of the wall will not qualitatively influence the onion to vortex transition, which is believed to be characteristic of narrow rings in the presence of a small asymmetry.

In our simulations we assumed a smooth, gradual variation of the ring width which acts as a smooth potential for the wall with an energy minimum at the narrow end, as illustrated in Fig. 4. This model leads to nucleation free switching as discussed above. To test this model further, we have performed simulations for rings with one small notch, representing the asymmetry, which traps one of the walls, leading to a nucleation free onion to vortex transition identical to that obtained for the smooth asymmetric ring. We infer that the exact nature of the asymmetry therefore does not influence the switching mechanism for the onion to vortex transition in these narrow rings, although the specific switching field is affected. In further support of our view that nucleation free switching occurs, we note that a nucleation process is very unlikely in the onion state: we have observed that the flux-closed part of the ring is stable up to the higher fields of the vortex to onion transition; also, nucleation in the remaining regions of the already existing domain walls is not energetically favorable nor likely to produce a vortex state. Finally we note the quantitative agreement between the values of the observed and the simulated switching fields and that the onion to vortex transition is observed to occur without any intermediate stable state.

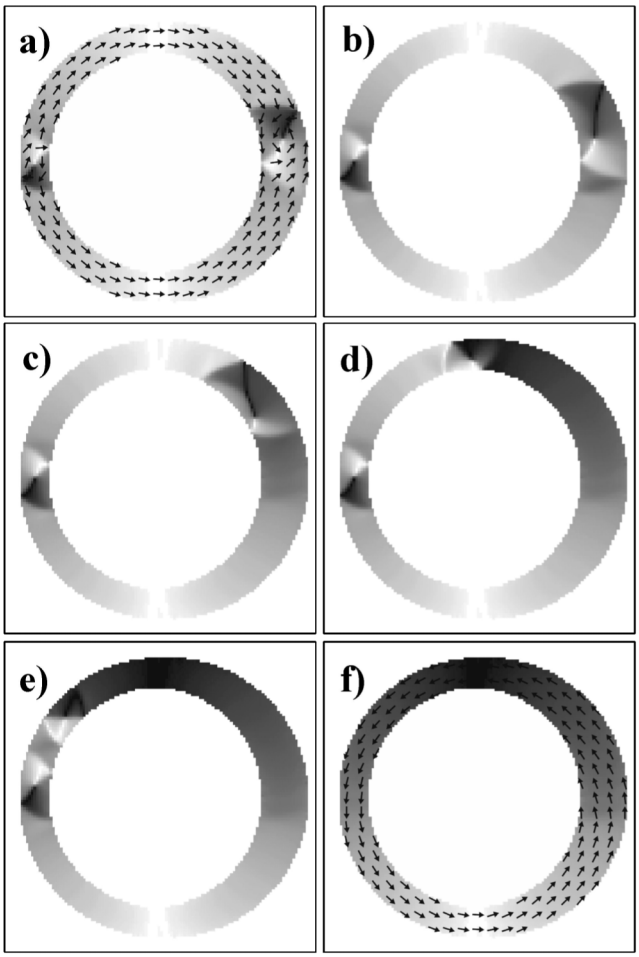

FIG. 4. Illustration of the onion to vortex switching in an asymmetric ring. The snapshots (a) and (f) are equilibrium states before and after the switching and snapshots (b) to (e) are intermediate states during the switching. The grey scale indicates the horizontal component of the magnetization in the plane, as illustrated by the arrows in (a) and (f).

This switching mechanism also provides an explanation for the observed relatively wide distribution of H_{C1}, considering the significant etch-induced edge roughness, illustrated in Fig. 1(a). As this edge roughness varies from ring to ring, the depinning field will therefore be ring dependent, giving rise to the observed distribution.

The second transition, vortex to onion, occurs by nucleation of a reversed domain in the half of the ring with magnetization antiparallel to the magnetic field, leading to two domain walls propagating to form a symmetric onion state. This transition has been described by Lopez-Diaz *et al.* [7], who demonstrate how the critical field for this transition can be tuned by varying the width and thickness of the rings. The nucleation of the reverse domains is initiated by the appearance of a vortex at the inner side of the ring. The nucleation field for this transition depends on the local curvature of the ring which explains the distribution of switching fields observed in Fig. 3. However, it should be stressed that we observe a good agreement between the results of the simulations and experiment.

In conclusion, we have discovered a well defined magnetic state in narrow magnetic rings which we term the onion state. The magnetic rings were prepared using prepatterned Si substrates to grow freestanding epitaxial elements of Cu(100)/Co(100)/Cu(100)/Si(100). The onion state was found to be stable up to an average applied field strength of 435 Oe, when it switches into the vortex state through a nucleation free domain wall motion. At about 1000 Oe, the rings switch into the reversed onion state via a more complicated nucleation-propagation process. The results show the importance of having well defined magnetic states in order to be able to predict the switching properties of an element, despite the presence of structural variations. The onion state has a limited stray field and can, under appropriate experimental conditions, be switched into the reversed onion state via the simultaneous movement of the domain walls, without any complicated intermediate states. Furthermore, for a precessional motion of the walls ultrafast switching on a subnanosecond scale is expected. The onion state could therefore be of importance for fundamental studies of magnetization dynamics, as well as providing a basis for ultrafast magnetic devices.

This work was supported by the European ESPRIT network MASSDOTS, the Portuguese PRAXIS XXI program (C. A. F. V.), and the European Commission (L. L.-D., EC HPMF-1999-00141).

[1] O. Fruchart *et al.,* Phys. Rev. Lett. **82**, 1305 (1999).
[2] R. P. Cowburn *et al.,* Phys. Rev. Lett. **83**, 1042 (1999).
[3] J. Yu *et al.,* J. Appl. Phys. **85**, 5501 (1999).
[4] E. C. Stoner and E. P. Wohlfarth, Philos. Trans. R. Soc. London, Ser. A **240**, 599 (1948).
[5] Y. Zheng and J. Zhu, J. Appl. Phys. **81**, 5471 (1997).
[6] T. Pokhil *et al.,* J. Appl. Phys. **87**, 6319 (2000).
[7] L. Lopez-Diaz *et al.,* IEEE Trans. Magn. (to be published).
[8] J. Zhu *et al.,* J. Appl. Phys. **87**, 6668 (2000).
[9] B. G. Demczyk *et al.,* J. Appl. Phys. **80**, 5035 (1996); J. Lee *et al.,* Phys. Rev. B **55**, 15 103 (1997).
[10] S.-M. F. Nee, Appl. Opt. **35**, 3570 (1996).
[11] R. D. McMichael and M. J. Donahue, IEEE Trans. Magn. **33**, 4167 (1997).